ENERGY BALANCE AND CO_2 EXCHANGE BEHAVIOUR IN SUB-TROPICAL YOUNG PINE (*Pinus roxburghii*) PLANTATION

Bimal K Bhattacharya[a,*], Nilendu Singh[b], Prafulla Soni[b] and J.S. Parihar[a]

[a]Earth, Ocean, Atmosphere, Planetary Sciences and Applications Area, Space Applications Centre (ISRO), Ahmedabad 380015, INDIA (bkbhattacharya@sac.isro.gov.in)
[b]Forest Ecology and Environment Division, Forest Research Institute, Dehradun 248006, INDIA (nilendu_singh@yahoo.com)

KEY WORDS: Micrometeorology, net photosynthesis, Chir pine forest, sub-tropics

ABSTRACT:

A study was conducted to understand the seasonal and annual energy balance behaviour of young and growing sub-tropical chir pine (*Pinus roxburghii*) plantation of eight years age in the Doon valley, India and its coupling with CO_2 exchange. The seasonal cycle of dekadal daytime latent heat fluxes mostly followed net radiation cycle with two minima and range between 50-200 Wm^{-2} but differed from the latter during the period when soil wetness and cloudiness were not coupled. Dekadal evaporative fraction closely followed the seasonal dryness-wetness cycle thus minimizing the effect of wind on energy partitioning as compared to diurnal variation. Daytime latent heat fluxes were found to have linear relationship with canopy net assimilation rate ($Y = 0.023X + 0.171$, $R^2 = 0.80$) though non-linearity exists between canopy latent heat flux and hourly net CO_2 assimilation rate . Night-time plant respiration was found to have linear relationship ($Y = 0.088 + 1.736$, $R^2 = 0.72$) with night-time average vapour pressure deficit (VPD). Daily average soil respiration was found to be non-linearly correlated to average soil temperatures ($Y = -0.034X^2 + 1.676X – 5.382$, $R^2 = 0.63$) The coupled use of empirical models, seasonal energy fluxes and associated parameters would be useful to annual water and carbon accounting in sub-tropical pine ecosystem of India in the absence high-response eddy covariance tower.

1. INTRODUCTION

More than half of the solar energy absorbed by land surfaces is currently used to evaporate water. Climate change is expected to intensify the hydrological cycle and to alter evapotranspiration, with implications for ecosystem services and feedback to regional and global carbon cycle. The changes in climatic conditions may significantly alter the greenhouse gas budgets and energy and water balances of natural ecosystems, forming a direct link between the global climate and biosphere (Piao et al., 2008). Forest ecosystem in sub-tropical climate is characteristically different from tropical and temperate forest ecosystems. It exchanges vast amounts of carbon, water and energy with the atmosphere and exhibits distinct seasonal trend and are thought to be important in controlling local and regional climates (Avissar and Pielke, 1991). Forests in sub-tropical and semi-arid regions of India are expected to be sensitive to greater climate variability such as changes in temperature, rainfall and seasonality. Long-term observations are not available by which changes in biodiversity due to observed changes in climate might be detected.

The Himalayan sub-tropical pine forest is the largest terrestrial eco-region in the Indo-pacific region and is spread over 3000 km at length occupying 76, 200 sq. km area. The chir pine (*Pinus roxburghii*) is the most dominant species distributed in four Indian states namely Uttarakhand, Himachal Pradesh, Jammu-Kashmir over western Himalaya and in Sikkim over eastern Himalaya. Pine forests are generally found at an elevation from 600 m to 1200 m. The functioning of Himalayan ecosystem , in particular, pine forests and the potential changes in their carbon, water and energy budgets are of particular importance because of their large extent and presumed sensitivity to climate variability and anthropogenic manipulations and disturbances. Today, large part of our knowledge on the complex multi-scale interactions between the climate and vegetation is based on models, whose major source of uncertainty can be traced back to the terrestrial biosphere and its processes (Denman et al., 2007). The Himalayan chir pine is closed-canopy system. The processes controlling the energy and carbon exchange in open-canopied pine ecosystems and scot pines (*Pinus sylvestris*) were studied by Anthoni et al (1999) and Launiainen (2011), respectively through measurements to understand, to predict the influences of climate on hydrology and productivity, and to improve atmospheric models relating exchange to surface conditions.

In the present study, we described seasonal variations of energy fluxes, evapotranspiration (expressed as latent heat flux, LE), CO_2 exchange rate over different phenological growth stages of young and growing sub-tropical chir pine. Therefore, The primary objectives are :

1) To characterize seasonal and annual variability of energy-water flux components over young and growing close-canopied pine forest system through observational records
2) Linking energy balance with biochemical processes in pine system

2. STUDY SITE AND DATASETS

The experimental site consists of young pine (8.5 years old) patch (500 m × 500 m) within the reserve pine forest (1.5 sq. km) of Forest Research Institute, Dehradun, in Doon valley of India (30°20′4″ N, 78°00′01″E, elevation : 640 m above MSL) constituted by Himalayan foothills in the north and Shivalik hills to the south. The site is surrounded by mature pine forest patches and managed grassland. Eighty year old pine forest exists to its eastern side. The young bamboo plantation forms its northern boundary; the southern side is bounded by mature mixed forest dominated by Sal and Teak. The land management practices generally allow to grow Lantana and other minor understorey species profusely. The average height of the young pines is ≈ 6.02 m which is increasing @ ≈ 0.37 m yr^{-1}. Mean diameter at breast height (DBH) is ≈ 13.23 cm which is increasing @ 1 cm yr^{-1}. Average crown height is about 3.56 m which is increasing @ ≈ 0.33 m yr^{-1}. Climatically, the site is in a subtropical system, a transition zone between temperate and tropical climate. The mean monthly air temperature averaged over twenty years was found to vary between 11.4˚C to 26.8˚C with the lowest in January and the highest during June. However, the mean monthly minimum air temperature varies between 3.9˚C to 22.7˚C and the maximum temperature varies between 19.8˚C to 33.9˚C. The mean monthly relative humidity averaged over twenty years was found to vary between 51.8% to 84.7% with the lowest in April and the highest in August. Minimum rainfall occurs in the month of November (≈3.67 mm) and maximum downpour occurs in the month of August (≈567.5 mm). Trend of bright sunshine hours averaged over twenty years was found to vary between 4.4 $hrsd^{-1}$ to 9.3 $hrsd^{-1}$ with minimum during the month of July and August and maximum during the month of May. The mean monthly open pan evaporation (mm) was found to vary between 35 mm to 216 mm with the lowest during December and highest during the month of May. Number of rainy days was maximum during the month of August (20) and minimum (1) during November / December.

The soil is deeply weathered mollisol and 3-8 m thick. The pH is in the range of 4.5 – 6.0, nutrient rich, with a porosity range of 40- 60%. The soil texture of the site is sandy clay loam with 35% sand, 40% clay and 25% silt. The bulk density of the soil is 1.03 because of high organic matter content.

A satellite-linked multi-layer micrometeorological tower of 13 m height was installed within young pine patch with a fetch ratio of approximately 1:50 for continuous and automated measurements of components of radiation balance (shortwave and longwave), Bowen Ratio Energy Balance (BREB) and water balance. The data were sampled at every 5 minutes and averaged over 30 minutes. Data logger automatically stored these data, which are retrieved and further processed to reproduce basic variables. These data were also uplinked to INSAT communication transponder through Yogi antenna with in-built Global Positioning System (GPS) and downlinked to earth station at Space Applications Centre (SAC), ISRO, Ahmadabad, India. Thus, in this study every half-hourly micrometeorological data were analyzed throughout a 13-month study period between March 2010 to March 2011.

3. METHODOLOGY

3.1 Bowen ratio energy balance (BREB)

The energy balance of a terrestrial surface may be expressed as

$$Rn - G = \lambda E + H \qquad (1)$$

Where, Rn is net radiation (Wm^2), G is the conductive soil heat flux (Wm^2), λE is the latent heat flux (Wm^2) where λ is the latent heat of vaporization of water ($2.45 x 10^6\ Jkg^{-1}$) and E is evaporation rate $(kgm^{-2}s^{-1})$ and H is sensible heat flux (Wm^{-2}). In this study, all terms except Rn are positive when the flow of energy is away from soil surface. The Bowen ratio is the ratio of the sensible to latent heat flux $(H / \lambda E)$ and is determined from differences in air temperature and vapour pressure of two heights.

$$\beta = \left[\frac{(\rho C_p)}{\lambda E}\right]\left(\frac{\Delta T}{\Delta e_a}\right)\left(\frac{K_h}{K_w}\right) \qquad \text{(Bowen, 1926)}$$

where β is the Bowen ratio, ρ is the atmospheric pressure (pa), C_p is the specific heat of air $(J\,kg^{-1}\,{}^oc)$, ε is the ratio of molecular weights of air and water, ΔT is air temperature difference $({}^o c)$, Δe_a is the vapour pressure difference (pa), K_h is the eddy diffusivity for heat $(m^2 s^{-1})$ and K_w is the eddy diffusivity for water vapour $(m^2 s^{-1})$. These two eddy diffusivities are same in similarity hypothesis with certain stability conditions of atmosphere.

Actual evapotranspiration in terms of energy flux is calculated as,

$$\lambda E = \frac{(Rn - G)}{(1+\beta)}$$

In pine, Bowen ratio was computed from the ratio of vertical gradients of air temperatures and actual vapour pressures (converted from relative humidity and air temperature data) between 2nd (7.5 m) and 3rd (12.5 m) height levels. Energy fluxes data were retained for daytime hours and filtered using the rejection criteria of Bowen ratios (Perez et al, 1999).

The batch processing of AMS data was carried out using 'Fluxsoft' software which was developed both in windows platform on Visual Studio as well as Linux platform using C++ using the protocol developed by Bhattacharya et al (2009). The first version computes radiative and convective fluxes using half-an-hourly datasets retrieved through datalogger and 'Agromet software utility 8.0'. The second version is applicable to data format of AMS received through satellite transmission.

Since, evapotranspiration from vegetation is negligible during nighttime, radiation and energy balance components were averaged for daytime hours for all the positive values of net radiation. An IDL (Interactive Data Language) routine was written to convert all half-an-hourly average fluxes into daytime averages. Ten-day (dekadal), fortnightly (15-day) and monthly averages of radiative and convective fluxes were made from daytime averages.

3.2 Field sampling plan

The rectangular experimental site was divided into nine (9) sampling quadrates (Figure 1). Four (4) in the east direction (named as EQ1 to EQ4), two (2) in the south direction (SQ1 and

SQ2), one each in the west and north direction (WQ & NQ) and central quadrat (CQ) taking consideration of the direction and space available. Central quadrat (CQ) is the exact point where micrometeorological tower is placed. The size of each quadrate was 10 m ×10 m.

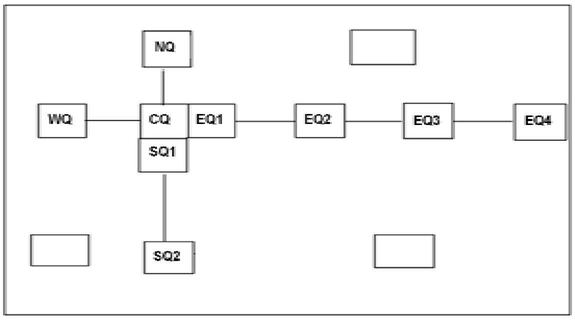

CQ : Central Quadrat, WQ : Western Quadrat, SQ : South Quadrat, NQ : North Quadrat

Figure 1. Sampling design for measurements biophysical properties and biochemical processes

3.2.1 **Green Leaf Area Index (GLAI) and green vegetation fraction (GVF):** Canopy analyzer LAI-2000 was used to measure needle leaf area index (LAI) at 10-day interval in all the nine quadrates. Each individual LAI value was recorded by taking eight readings (two readings above the canopy and six readings below the canopy in different directions) followed by averaging. The individual LAI values were averaged over the number of trees in respective quadrates. The mean LAI was computed by considering the LAIs of all the quadrates. LAI sampling was done in the absence of direct sunlight either in fully cloudy day or at the time of dusk. Gower and Norman (1990) hypothesized that LAI-2000 is actually measuring a “shoot area index” (SAI) in conifers, rather than a “needle area index” and proposed correcting the LAI-2000’s prediction by multiplying them with a correction factor (R).

R = Projected needle area / Average projected shoot area

The R-value for each plant was computed by averaging three values of each branch representing three levels of nodes i.e. lower, middle and upper. One branch from each level of node was cut and R-value was computed individually. The computed R-value in the present case was found to be 1.57.

All the plants in each quadrate were grouped into different ‘crown height range’ classes such as 1-2 m, 2-3 m, 3-4 m, 4-5 m, 5-6 m. Architecture of the canopy is such that the crown was divided into three levels on the basis of positions of nodes : lower, middle and upper levels. For counting the total number of needles in each level of a plant (e.g. lower, middle & upper), a branch was cut from each level and total number of fascicles in that branch was manually counted, multiplied by 3 to get the total number of needles in that branch (since each fascicle contains three needles). Finally, the total needle count in that branch was further multiplied by total number of branches to obtain the total number of needles in that level. Needle length and diameter were measured with measuring scale and digital calipers and corresponding average values were considered. All these values (e.g. needle count, length, diameter etc.) were utilized to calculate total surface area at each level and an average surface area was taken accordingly for the whole crown. This process was repeated for all crown height range classes.

However, the green surface area values can be considered till September end only, since leaf browning starts from first week of October and continues upto December followed by needle drying (January to December). The period between March to May corresponds to elongation and needle greening, followed by 100% green needles between June to September characterized by fully green and mature, elongated needles. During this period, total photosynthetic area (computed by mechanical counting of all needles in the crown) was equated with GVF of value one (1) representing 100% GVF. In the first week of October, traces of brown needles began to appear. By the end of October, about 5% of the needles turned brown. Thus, GVF at the end of October was 0.95. As plants progressively entered into physiologically dormant stage with the approach of winter, the rate of browning increased rapidly. At the end of each month remaining green needles were counted manually and GVF were calculated accordingly. By the end of March, about 7- 8 % of the leaf remained green. So, GVF at this stage was about 0.075. The month of March was also characterized by simultaneous emergence of new, elongating needle buds. The computation of total photosynthetic surface area and Green Vegetative Fraction (GVF) were continued between period of March to May.

3.3 Carbon Absorption Potential (CAP)

Carbon Absorption Potential (CAP) of a vegetative system can only be represented by its Net Primary Productivity (NPP).

Daily (NPP_d) is generally computed by subtracting the daily sum of day and night-time plant respiration (Rd_{day} & Rd_{night}) from daily gross photosynthetic assimilation or gross primary productivity (GPP_d)

$$NPP_d = GPP_{day} – (Rd_{day} + Rd_{night}) \qquad (2)$$

Photosynthesis data averaged over daytime hours by LI-6400 XT portable photosynthesis system (LICOR) represents daytime net photosynthetic assimilation (Ac_{day}), which is (GPP_{day}) minus daytime plant respiration (Rd_{day}).

$$Ac_{day} = GPP_{day} - Rd_{day} \qquad (3)$$

Night-time averages of measurements from LI-6400 XT represents night-time plant respiration (Rd_{night}). Thus, daily NPP (NPP_d) was computed by subtracting the night-time plant respiration (Rd_{night}) from daytime net photosynthetic assimilation (Ac_{day})

$$NPP_d = Ac_{day} - Rd_{night} \qquad (4)$$

Instantaneous leaf assimilation rates were converted to canopy assimilation rate (A_c) using sunlit canopy and mean tilt angle as given below.

LI-6400-XT portable photosynthesis system (LICOR) was utilized to measure leaf level photosynthetic rate and night-time plant respiration rate. The LI-6400 is an open system, the measurements of photosynthesis / respiration are based on the differences in CO_2 in an air stream that is flowing through the leaf cuvette. These data were collected from November 10, 2010 to

April 10, 2011, regularly at 10-day interval, three times in a month. Data were collected every hour throughout the day and night. Needles of each level of nodes were covered along the four directions. Thus, for storing photosynthetic and respiration data of each hour, 8-12, two (2) minutes' readings were taken and averaged for that hour. Soil respiration was simultaneously measured throughout day and night using a soil respiration chamber.

4. RESULTS AND DISCUSSION

4.1 Seasonal variation of energy balance components

The seasonal behaviour of daytime average energy balance components such as net radiation and latent heat fluxes in Chir pine are shown in Figure 2.

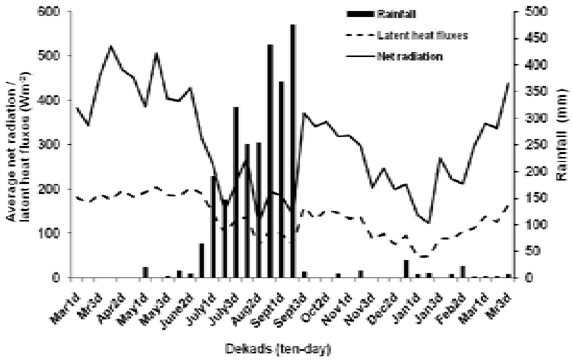

Figure 2. Seasonal behaviour of energy balance components Young Chir pine plantation

The Bowen ratio was found to vary between 0.5 to 3.0 with the low magnitude during monsoon months coincident to wet spells associated with rain and higher values during spring-summer months. Similar range and seasonal trend of monthly average Bowen ratio between 0.23 to 3.25 was also noticed in pine system by Sun et al (2010). The latent heat fluxes were found to be the highest (200 Wm^{-2}) during spring-summer months due to high net radiation (500 Wm^{-2}) because of relatively clear skies but with intermittent drizzle. In the monsoon months, latent heat fluxes became very low (70-80 Wm^{-2}) due to low evapotranspiration rates owing to the persistent cloud cover thereby cutting the net radiation to the level of 150 Wm^{-2}. A secondary peak (375 Wm^{-2}) was noticed in the autumn when there was a falling seasonal limb of net radiation but with relatively clear skies. This corresponded to fully green-up stage of pine. During winter (November onwards), latent heat fluxes started decreasing which corresponded to initiation of browning stage. It became the lowest (50 Wm^{-2}) during January corresponding to complete browning and drying stage of needles (dormant stage). This period was also marked by exposure to low radiation and temperatures (minimum temperatures about 2.5°C and low diurnal temperature range). The limitation of both radiation and temperature restricted active growth of pine and thereby transpiration. Again, with increase in temperature and radiation level, active growth started towards spring-summer with intermittent rainfall leading to greening. This caused evapotranspiration rates to be higher. Wider difference between trends of net radiation and latent heat fluxes was found during pre-monsoon and post-monsoon periods having less occurrence cloudy skies. During south-west monsoon period both are low but nature of variability is closely resemble each other majorly influenced by the presence of persistent cloudy conditions.

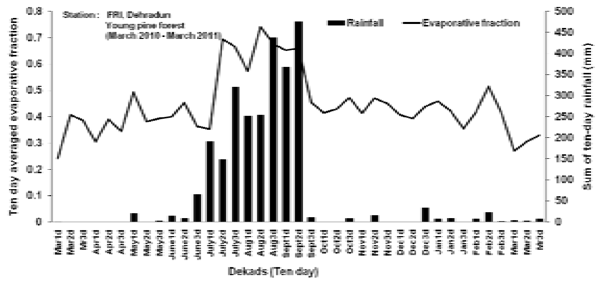

Figure 3. Seasonal variation of evaporative fraction

The plot of day-time averaged evaporative fraction ($\frac{1}{1+\beta}$ or $\frac{\lambda E}{H+\lambda E}$) and sum of ten-day rainfall showed that evaporative fraction varied between 0.23 to 0.75 (Figure 3) throughout the pine growth cycle.

In the summer-monsoon season coincident to maximum green-up stage of pine (July1d to Sept2d) and rainfall between 150 to 450 mm, evaporative fraction showed a substantial increase to around its maximum possible theoretical limit of unity with the intermittent lowering depending on the level of decrease of dekadal cumulative rainfall. In the remaining part of the growth cycle, evaporative fraction showed a systematic decline with intermittent increase caused by occurrence of rainfall. Though instantaneous and diurnal evaporative fraction are influenced by radiative forcing, soil wetness and wind turbulence forming stability and in-stability, the averaging over ten-days or a fortnight made the evaporative fraction more sensitive to soil wetness for same level of radiative forcing nullifying the effect of frequent wind fluctuations.

4.2 Empirical models of daytime canopy net CO_2 assimilation (Ac_{day}), night-time plant respiration (Rd_{night}) and daily soil respiration (Rd_{soil})

The variation of leaf and canopy net CO_2 assimilation rates were found to be almost similar and the magnitudes were very close to each other between (1.2 to 2.8 μmol CO_2 $m^{-2}s^{-1}$) when needle browning took over followed by drying up to Jan1d. As greening started, both showed an increasing trend but daytime average leaf assimilation rate became higher (1.2 to 5.5 μmol CO_2 $m^{-2}s^{-1}$) than canopy assimilation rate (1.2 to 3.0 μmol CO_2 $m^{-2}s^{-1}$) and the difference was widened with the higher level of greening. Higher rate of increase was found for leaf than canopy. Canopy assimilation represents photosynthesis from sun-lit portion of canopy but whole green leaf area is represented in case of leaf assimilation rate. A linear relationship ($Y = 0.023X + 0.171$, $R^2 = 0.80$) was found to exist between daytime average latent heat fluxes and canopy net assimilation rate (Figure 4a). Latent heat fluxes were partitioned into canopy component using GVF. The plot of instantaneous canopy net assimilation rate and canopy latent heat fluxes at ten-day interval for a range of GVF (0.09 to 0.9) showed differential response (Figure 4b) to canopy latent heat fluxes at high to low GVF levels.

The non-linearity in their relations were systematically overtaken by linearity as GVF decreased. In tall forest vegetation, canopy with higher foliage fraction with vertical and three-dimensional distribution holds moisture either intercepted by rainfall or dew or fog that possibly forms a temporary thin film. As compared to short vegetation, the evaporation from different vertical strata becomes a major contributor to canopy component of latent heat fluxes in addition to transpiration in tall forest vegetation. The latter component mainly depends on soil water availability, plant water uptake and atmospheric vapour pressure deficit coupled with stomata down-regulation. Therefore, canopy latent heat fluxes at low GVF represented more of transpiration and hence showed strong linear relation with photosynthesis or canopy net assimilation rate. Moreover, at higher GVF, the thin moisture layer surrounding green foliage might partially restrict vapour transfer through transpiration and also CO_2 intake. This could also lead to more of non-linear situation. In addition to that, profuse growth of understorey vegetation coincident to higher pine GVF might also contribute to overall latent heat fluxes. This component could become negligible towards October-November with the man-made clearing of understorey when pine GVF was also low.

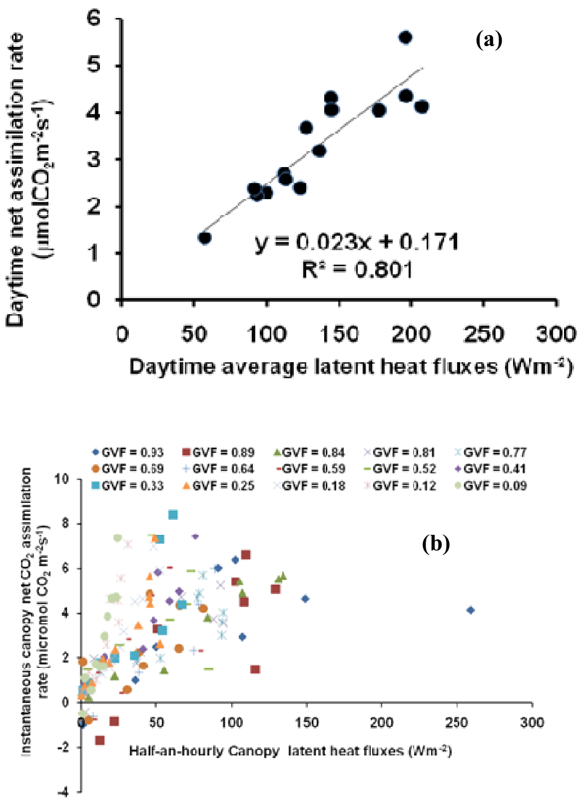

Figure 4. Latent heat fluxes vs. photosynthesis for (a) daytime average and (b) for diurnal instances at different green vegetation fraction (GVF)

It can be concluded that three sources of latent heat fluxes obtained from micrometeorological data need to be resolved instead of two sources to model canopy transpiration and net assimilation rate or water use efficiency in tall vegetation including pine. However, the existence of non-linearity seemed to be averaged out for daytime averages.

Though effect of weather parameters specially air and soil temperatures on pine maintenance (Ryan and Waring, 1992), dark respiration (Ryan et al, 1994) and soil respiration (Xue et al, 2007) was studied, but species-specific models have not been reported so far. The average night-time plant respiration rate was found to have strong linear relation ($Y = -0.088X + 1.736$, $R^2 = 0.72$) with average night-time Vapour Pressure Deficit (VPD) from AMS measurements (Figure 5a) among different other variables. Daily average soil respiration rate was found to have second-order polynomial relation (Figure 5b) with average soil temperature between 0 to 30 cm ($Y = -0.034X^2 + 1.676X – 5.382$, $R^2 = 0.63$).

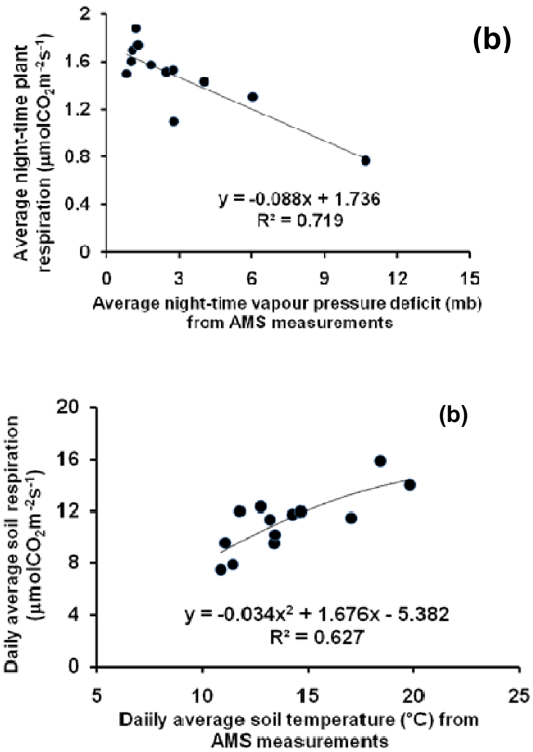

Figure 5. Relations of (a) night-time plant respiration and (b) soil respiration with micrometeorological variables

5. CONCLUSIONS

Dekadal evaporative fraction more or less represented surface wetness pattern with substantially higher magnitude during summer-monsoon followed by low level in the spring-summer as well as autumn-winter. Intermittent fluctuations were also caused by intermittent variations in rainfall. Though linear relations were found between daytime latent heat fluxes and canopy net assimilation rate, but more non-linearity tends to exist between canopy component of hourly latent heat fluxes and hourly canopy assimilation rate at higher green fraction of pine. This could be due to presence of additional sources of latent heat fluxes from water held in thin film on the needles in different vertical strata and contribution from understorey species. Both of these faded out towards post-monsoon with lesser green fraction in pine and understorey. Nigh-time plant respiration and daily soil respiration could be modeled by night-time VPD and daily average soil temperature with linear and second-order polynomial relation, respectively. These empirical models would be useful to fill-up gaps in seasonal and annual carbon accounting in absence of 'high response' eddy covariance but in presence of 'slow response' Bowen ratio system. These models have the scope of upscaling for extrapolation to large pine based ecosystems using similar spatio-temporal data fields of latent heat fluxes, VPD and soil temperatures either generated through remote sensing observations or high resolution model simulation. Moreover, the observational evidences of inter-relations among parameters and processes would be able to provide insight on how a growing pine will respond to changing climate scenarios.

REFERENCES

Anthoni, P. M., Law, B.E., Unsworth, M.H. (1999). Carbon and water vapor exchange of an open-canopied ponderosa pine ecosystem. *Agricultural and Forest Meteorology*, 95, pp. 151-168

Avissar, R., Pielke, R.A. (1991). The impact of plant stomata control on mesoscale atmospheric circulations. *Agricultural and Forest Meteorology* 54, pp. 353-372

Bhattacharya, B. K., K. Gunjal, Nanda, M. and Panigrahy, S. (2009). Protocol Development of Energy-Water Flux Computation from AMS and Model Development. *SAC/RESA/ARG/EMEVS/SR/02/2009*, Chapter 3, pp 34-53

Bowen, I. J. (1926). The ratio of heat losses by conduction and by evaporation from any water surface. *Physical review*, 27, pp. 770-787

Denman K.L. et al., in Climate Change 2007: The Physical Science Basis. Contribution of Working Group I to the Fourth Assessment Report of the *Intergovernmental Panel on Climate Change*. Solomon S. et al., (eds.). Cambridge Univ. Press, Cambridge, pp. 499–587.

Gower, S.J. and Norman, J.M. (1990). Rapid estimation of leaf area index in forests using the LI COR LAI 2000. *Ecology*. 72, pp. 1896-1900

Launiainen, S. (2011). Canopy processes, fluxes and micro-climate in a pine forest. In : *Report series in Aerosol Science, No. 117*, Division of Atmospheric Sciences, Department of Physics, Faculty of Science, University of Helsinki, Helsinki, Finland Academic dissertation

Monteith, J.L. and Unsworth, M. (2008). *Principles of Environmental Physics* (third edition). ISBN 978-0-12-505103-3

Perez, P.J., Castellvi, F., Ibanez, M., Rosell, J.I.,1999. Assessment of reliability of Bowen ratio method for portioning fluxes. Agric. For. Meteorol., 97, pp. 141–150.

Piao, S.L., Ciais, P., Friedlingstein, P., Peylin, P., Reichstein, M., Luyssaert, S., Margolis, H., Fang, J.Y., Barr, L., Chen, A.P., Grelle, A., Hollinger, D., Laurila, T., Lindroth, A., Richardson, A.D. and Vesala T. (2008). Net carbon dioxide losses of northern ecosystems in response to autumn warming, *Nature*, 451, pp. 49 52

Ryan, M.G., Limber, S., Vose, J.M. and Hubbard, R.M. (1994). Dark respiration of pines. *Ecological Bulletins*, 43, pp. 50-63

Ryan, M.K. and waring, R.H. (1992). Maintenance respiration and stand development in a subalpine lodgepole pine forest. *Ecology*, 73(6), 2100-2108

Sun, G., Noormets, A.,Gavazzi, , M.J., Mcnulty, S.G., Chen, J., Domec, J.C., King, J.S., Amatya, D.M., Skaggs, R.W. (2010). Energy and water balance of two contrasting loblolly pine plantations on the lower coastal plain of North Carolina, USA. *Forest Ecology and Management*, 259, pp. 1299-1310

Xu, W., Gungang-Sheng, Z., Yan-Ling, J., Chang-Ming, C., Wei, Z., Jian, S. (2007). Soil respiration in a clear-cut broad-leaved Korean pine forest of Cahngbai mountain. *Chineese Journal of Plant Ecology*, 31(3), pp. 355-362

ACKNOWLEDGEMENTS

This study was carried out in the ISRO-GBP project titled "Energy and Mass Exchange in Vegetative Systems". We are thankful to Dr. R. R. Navalgund, Director, Space Applications Centre (ISRO), Ahmedabad and Dr. S.S. Negi, Director, Forest Research Institute, Dehradun for their constant support and encouragement. The first three authors are grateful to Dr. Sushma Panigrahy, Group Director, ABHG and Dr. S.S. Ray, Head, AED for giving time to time guidance while carrying out the work.